IEEE Access
Multidisciplinary | Rapid Review | Open Access Journal

Received March 10, 2019, accepted April 9, 2019, date of publication April 29, 2019, date of current version May 20, 2019.

Digital Object Identifier 10.1109/ACCESS.2019.2913558

Characteristics of the Flexible Graphite Grounding Material and Its Engineering Application

DAOCHUN HUANG, (Senior Member, IEEE), JUN XIA, JIANGJUN RUAN, (Member, IEEE), YONGCONG WU, AND WANLIN QUAN

School of Electrical Engineering and Automation, Wuhan University, Wuhan 430072, China

Corresponding author: Daochun Huang (huangdc99@163.com)

This work was supported by the Natural Science Foundation Innovation Group Program of Hubei Province China under Grant 2016CFA007.

ABSTRACT In order to meet the requirements of corrosion resistance of the grounding material and thermal stability of the grounding material of the transmission line towers, under the condition of power frequency current and high-frequency lightning current scattering into the ground in the case of short-circuit fault and lightning strikes, a kind of high-current capability flexible graphite grounding material was developed. The corrosion resistance of the flexible graphite grounding material and the steel type grounding material was compared by the soil simulation solution corrosion tests. The contact performance with different soils of the two materials was analyzed by the actual contact resistance measurement test. The thermal stability and the impulse current effective length of this grounding material were studied by means of simulation calculation. The results show that the high-current capability flexible graphite grounding material has a strong anticorrosion characteristic, whose reliable service life can exceed 30 years. Compared to the round steel grounding material, the contact resistance with the soil can be reduced by approximately 30%, and the impulse current effective length can be increased by about 30%.

INDEX TERMS Flexible graphite grounding material, corrosion resistant characteristic, contact resistance, thermal stability, impulse current effective length.

I. INTRODUCTION

With the continuous development of the power grid, the requirement for safe and stable operation of transmission lines is also increasing. The lightning stroke fault of the transmission line is the first major factor threatening the stable operation of the transmission lines [1], [2]. Most tropical countries, several southern states of the United States, several regions of Japan, China and Australia, experience heavy annual lightning occurrence density [3], [4]. With the continuous improvement of lightning protection technology, engineers and researchers had conducted in-depth research on the transient characteristic of lightning strike [5], [6]. According to the operation experiences, reliable grounding was one of the keys to lightning protection of the overhead transmission line. The low-resistance, long-term and stable grounding device was an important guarantee for safe and stable operation of the power system [7].

For a long time, copper, steel, and other metal materials had been the main materials of the power system grounding device [8]. However, there was a serious corrosion phenomenon of the traditional steel grounding material buried in the soil for a period of time, which had also become a bottleneck problem affecting its service life [9], [10]. Due to the large elastic modulus of metal type grounding materials and their intrinsic incompatibility with the plasticity of the soil, the effect of electrical "connection" was poor; the steel type grounding material with large relative magnetic permeability had serious inductance effect in large-scale grounding grids. The problem of the impulse current effective length of the grounding electrode when flowing through high frequency lightning current had not attracted sufficient attention.

Aiming at the corrosion problem of the steel grounding material in engineering, some non-metal grounding materials had emerged, of which one of the most widely used was the flexible graphite grounding material [11]–[13]. However, the power frequency short-circuit current of the transmission line also need to pay more attention. The short circuit current value flowing through the faulty tower can reach hundreds or even thousands amperes. Its ability to withstand the power frequency short circuit current of the transmission line remains to be improved.

In order to solve the existing problem and provide a better guarantee for the safe and stable operation of

The associate editor coordinating the review of this manuscript and approving it for publication was Ildiko Peter.

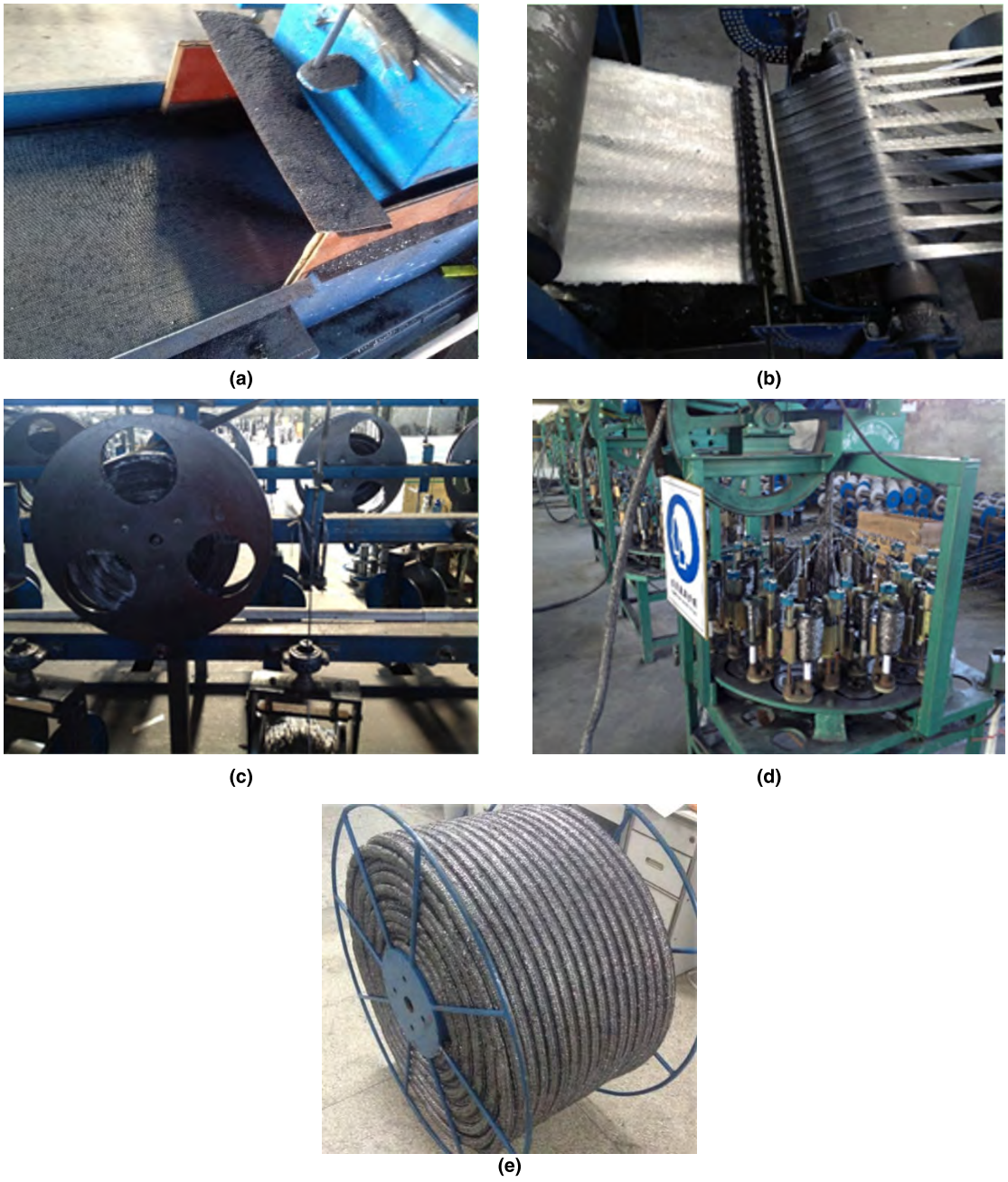

FIGURE 1. Pictures of the actual productive process. (a) Rolling of the graphite paper. (b) Cutting into slim. (c) Twisting into the graphite wire. (d) Weaving into the graphite grounding material. (e) The finished flexible graphite grounding material.

transmission lines, a kind of high current capability flexible graphite grounding material was developed. Firstly, this paper introduced the preparation progress and structure of this material. Secondly, its contact performance, corrosion resistance, thermal stability and impulse current effective length were studied by comparison and analysis with the traditional steel grounding material. Finally, the practical application effect of this material was analyzed combining with the actual grounding engineering.

II. PREPARATION PROGRESS AND STRUCTURE

The raw material of this material includes high-purity crystalline flake graphite, chemical fiber, adhesive, conductive adhesive and copper wire. Among them, the purity of the crystalline flake graphite should meet the requirement of not less than 95%. The chemical fiber was used to enhance the mechanical properties, the tensile strength of the chemical fiber should be greater than 2 GPa, and which should also has the characteristic of corrosion resistance and easy processing. The adhesive was used to hold the graphite paper and the chemical fiber. The conductive adhesive and copper wire were used to enhance the overall electrical conductivity of this material.

This material adopted reinforced fiber as the skeleton, and the high-purity expanded graphite was used as the main body. It was pressed after being coated with the adhesive, and the

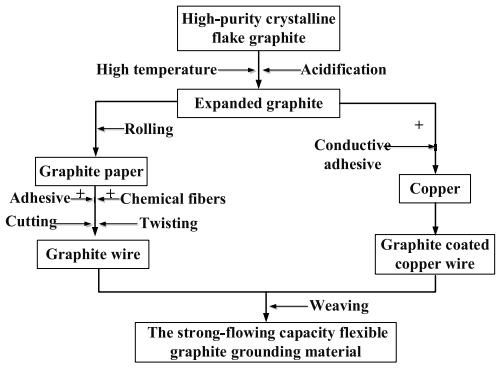

FIGURE 2. Flow chart of the productive process.

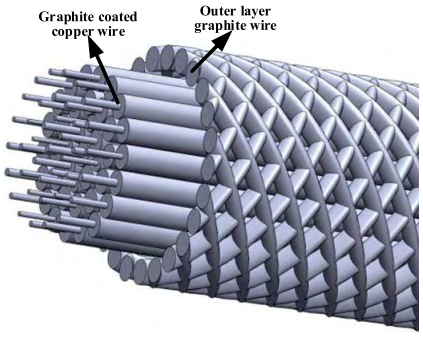

FIGURE 3. Structural diagram of the high current capability flexible graphite grounding material.

high-density and high-conductivity flexible graphite grounding material was obtained finally. The general preparation progress of this material as follows:

(1) Expanded graphite was produced by the high-purity crystalline flake graphite after high temperature and acidification.

(2) Then the graphite paper can be obtained by rolling the expanded graphite.

(3) The two layers of the graphite paper and chemical fibers were tightly bonded and pressed together by the adhesive through dipping process and heat curing process.

(4) The two layers structure of the graphite paper was cut into fine filaments with the same width, then the filament was twisted into the graphite wire.

(5) The conductive adhesive was used for coating the graphite evenly, tightly and integrally on the surface of the copper wire, which we call it graphite-coated copper wire.

(6) Finally, the high current capability flexible graphite grounding material was woven with the graphite wire and graphite coated copper wire.

The picture and flowchart of the productive process are shown in Figure 1 and Figure 2.

The structure schematic of the high current capability flexible graphite grounding material is shown in Figure 3.

In the structural design of the flexible graphite grounding material, reference was made to the structural principle of the *Litz* line (German: Litze Draht, meaning ''woven line''). The structure of the graphite flexible grounding material was established by combination of the graphite-coated copper wire and toughened flexible graphite wire, and considering the layout of flowing-current conductor and scattering-current surface.

The inner layer of the material was uniformly arranged by a plurality of the graphite wire and graphite-coated copper wire. The outer graphite wire was woven from the graphite wire.

Through this structural design, the skin effect and inductance effect of the grounding material under the action of high frequency lightning current or short circuit current can be effectively reduced.

TABLE 1. The soil simulation solution of the grounding material corrosion tests.

Soil simulation solution number	Soil type	Mass concentration (g/L)			pH
		NaCl	Na_2SO_4	$NaHCO_3$	
A	Chlorinated saline soil	18.040	1.660	/	8.80
B	Saline-alkali soil	1.810	17.740	/	8.60
C	Meadow soil	0.028	0.190	0.110	7.40
D	Red soil	0.138	0.080	0.014	4.40
E	Strong acid soil	0.145	0.060	0.010	3.10

III. GROUNDING CHARACTERISTICS

A. SOIL SIMULATION SOLUTION CORROSION TEST

According to the different pH of the soil, it can be divided into acidic soil, neutral soil and alkaline soil. In order to further analyze the corrosion resistance of the high current capability flexible graphite grounding material, the corrosion rate was measured by using soil simulation solution corrosion test.

In the test, distilled water was used to prepare the salt solution. At the same time, the pH of the soil simulation solution was adjusted by Acetic Acid and Sodium Hydroxide. The soil simulation solution of the corrosion resistance test is shown in Table 1.

The corrosion test samples of the Q235 carbon steel and the flexible graphite grounding material of the same size were prepared. Those test samples were put into the five soil simulation solutions with the above pH values of 3.10 to 8.80 respectively to simulate different soil corrosion conditions. The diagram of the soil simulation solution corrosion test is shown in Figure 4. In order to eliminate the error, a parallel test method was used to measure the corrosion resistance of the two materials respectively. In the process of corrosion resistance tests, attention should be paid to the change of the soil simulation solution level in each container, which should be replenished in time to the initial level. The corrosion resistance tests lasted for 190 days.

Before starting the test, drying the test samples, the weight of those test samples was weighed using an analytical balance with an accuracy of 0.1 mg, and the corresponding data was recorded. When the test was completed, those test samples in different soil simulation solutions were washed

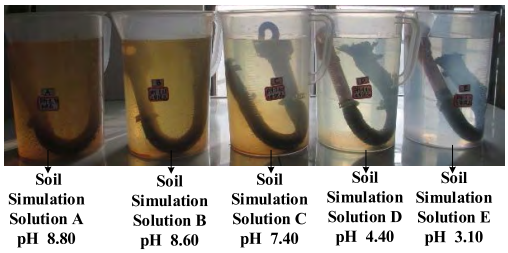

FIGURE 4. Diagram of the soil simulation solution corrosion tests.

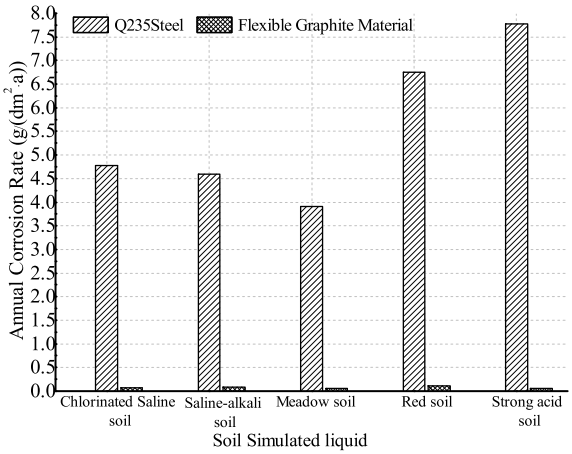

FIGURE 5. The annual corrosion rate of the two grounding materials.

with the deionized water. The corrosion layer on the surface of the steel sample was wiped off with a rust remover, and cleaned again with Acetone. After drying, the weight of those test samples were weighed again by analytical balance. By using the weight loss method to measure the corrosion rate of the grounding material before and after the corrosion test. Calculating the corrosion rate is shown in equation (1).

$$v_w = \frac{\Delta w}{S \cdot t} = \frac{|w - w_0|}{S \cdot t} \tag{1}$$

where v_w is the corrosion rate of the test samples; S is the area of the test samples; t is the test time; w_0 and w are the weight of the test samples before and after the test.

The annual corrosion rate of the two grounding materials is shown in Figure. 5. The results showed that annual corrosion rate of the high current capability flexible graphite grounding material was about 0.13 g/(dm^2·a), which was much lower than that of the Q235 carbon steel. The high current capability flexible graphite grounding material was not limited by the soil conditions, its corrosion resistance was significantly better than that of the steel grounding material, whose reliable service life can exceed 30 years.

B. CONTACT PERFORMANCE WITH THE SOIL

The actual grounding engineering design was based on that the grounding material was ideal contact with the soil, however the contact resistance had not attracted enough attention, and the accurate estimation of the grounding resistance margin was lacking. It was easy to appear that the actual grounding construction was difficult to meet the requirement of design standards in special soil areas (such as rock areas and permafrost areas). Therefore, the contact performance with the soil between the round steel and the high current capability flexible graphite grounding material was analyzed through a comparison test.

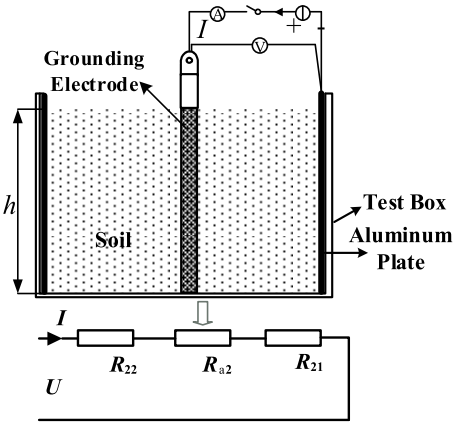

FIGURE 6. The measurement method diagram of the contact resistance.

1) MEASUREMENT METHOD

When measuring the contact resistance of the grounding electrode with the soil, the single side aluminum plate can be used as the return electrode of the current by injecting the AC current into the grounding electrode. The measurement principle diagram can be equivalent to a series circuit made up of the contact resistance R_{22} between the grounding electrode and the soil, the soil resistance R_{a2}, the contact resistance R_{21} between the aluminum plate and the soil. The measurement method diagram as shown in Figure 6.

The total resistance R of the circuit can be calculated in equation (2).

$$R = \frac{U}{I} = R_{22} + R_{a2} + R_{21} \tag{2}$$

where U is the voltage measured between the grounding electrode and the aluminum plate; I is the total current flowing through the circuit.

The soil resistance R_{a2} can be calculated by using the finite element method.

$$I^2 \cdot R_{a2} = \sum W_i \tag{3}$$

where W_i is the thermal power of the number i soil unit volume.

The contact resistance R_{21} between the aluminum plate and the soil can also be derived by using the finite element method.

$$I^2 \cdot R_{21} = \sum I_i^2 \cdot R_{01}/S_i$$
$$R_{21} = \frac{\sum I_i^2 \cdot R_{01}/S_i}{I^2} \tag{4}$$

TABLE 2. The mass ratios of different soil conditions.

Soil type	Loess	Fine sand	Bentonite	10 mm Gravel	20 mm Gravel
Type 1	100%				
Type 2		100%			
Type 3			100%		
Type 4	50%	25%		25%	
Type 5	50%	25%			25%
Type 6	25%		25%	25%	25%
Type 7		40%	20%	20%	20%
Type 8				50%	50%

where R_{01} is the contact resistance between the aluminum plate and the soil of per unit area; S_i is the area of the aluminum plate unit i.

From equation (2) to (4), we can know that the contact resistance between the grounding electrode and the soil can be calculated with equation (5).

$$R_{22} = R - R_{a2} - R_{21} \tag{5}$$

2) CONTACT PERFORMANCE TEST

In order to measure the contact resistance of the high current capability flexible graphite grounding material under different soil conditions and compare it with the round steel grounding material, both the two materials with a diameter of 28 mm were used as the research objects. (The steel with a diameter of 28 mm was not used frequently in actual grounding engineering, but in order to ensure the consistency of the contact area between the grounding electrode and the soil, choosing the grounding material of the same diameter.)

In order to simulate different soil conditions, the tests were carried out under eight soil conditions respectively, and the specific mass ratios of the soil condition are shown in Table 2.

The measurement of the contact resistance was carried out in an organic glass box with a length, width and height of 300 mm × 200 mm × 200 mm. A circular hole with a diameter of 29 mm was located at the center of the bottom plate to ensure that the grounding electrode was arranged at the center of the test box. The left and right sides of the test box were the aluminum plate of 200 mm × 200 mm × 2 mm, which served as the current injection and return electrode respectively. The layout of the test platform is shown in Figure 7.

The calculation of the contact resistance between the grounding electrode and the soil needs to be completed with four steps: firstly, placing the grounding electrode in the test box and filling in different soils, then connecting the test circuit; secondly using the four-electrode method to measure the soil resistivity; thirdly the soil resistance R_{a2} and the contact resistance R_{21} between the aluminum plate and the soil were equivalently calculated based on the finite element method; finally, the grounding electrode was used as the current injection electrode, and the single-sided aluminum plate was used as the current return electrode. The contact resistance R_{22} of per unit area between the grounding electrode and the soil can be calculated from equation (3) to (6). The contact resistance of per unit area of the grounding electrode under different soil conditions is shown in Table 3.

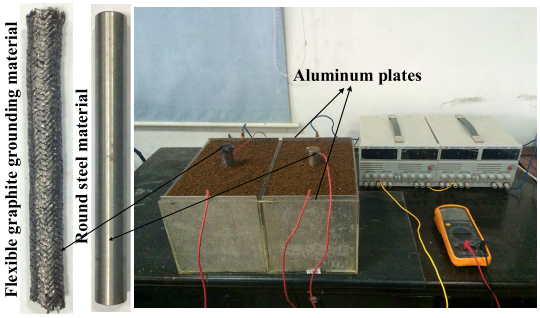

FIGURE 7. Layout diagram of the actual test platform.

TABLE 3. Contact resistances of the two grounding materials.

Soil type	Grounding electrode	Soil resistivity (Ω·m)	Contact resistances of per unit area (Ω/ m^2)
1	Graphite	267.52	0.58
	Steel	266.05	1.56
2	Graphite	1 791.23	8.10
	Steel	1 753.92	18.99
3	Graphite	9.80	0.021
	Steel	9.55	0.016
4	Graphite	697.99	1.19
	Steel	709.47	3.42
5	Graphite	779.9	2.78
	Steel	802.76	6.37
6	Graphite	96.68	0.16
	Steel	98.46	0.30
7	Graphite	171.36	0.29
	Steel	169.55	0.56
8	Graphite	4 405.98	25.73
	Steel	4 344.21	79.79

The actual measurement results showed that when the soil particle size was very small and the resistivity was low, it can be considered that the contact resistance of per unit area of the two materials was almost the same. When the soil particle size was large and the soil resistivity was high, the contact resistance of per unit area between the grounding electrode and the soil can not be ignored.

According to the contact resistance test results of the eight different soil conditions, it can be seen that the contact resistance of per unit area of the flexible graphite grounding material can be reduced by about 30% on average compared to the round steel material.

C. THERMAL STABILITY

In order to compare and analyze the thermal stability of high current capability flexible graphite grounding material and

TABLE 4. Parameters of different grounding materials.

Parameters	Resistivity (Ω·m)	Relative permeability	Specific heat capability (J/(kg·K))	Thermal conductivity (W/(m·K))	Mass density (kg/m^3)
Graphite	5×10^{-7}	1	710	129	2000
Steel	1×10^{-7}	636	460	45	7800

TABLE 5. Calculation of impedance and temperature rise of different grounding materials.

Grounding materials	Grounding impedance at different frequencies (mΩ)			Temperature rise under a short circuit current of 3 kA/1 s (C)
	DC	50 Hz	10 kHz	
Round steel	1.27	4.81	64.04	181.7
Flat steel	1.25	3.16	45.49	133.5
Flexible graphite grounding material containing 9 copper wires	1.25	1.25	1.38	14.6
Flexible graphite grounding material containing 16 copper wires	1.22	1.22	1.30	13.7

steel grounding electrode under flowing through the same current condition. The finite element method was used to calculate the grounding impedance of the grounding material at different frequency currents and the temperature rise under the action of a short circuit current of 3 kA/1 s. The parameters of the two grounding materials are shown in Table 4.

The research objects selected the round steel with a diameter of 10 mm, the flat steel with a cross section of 20 mm × 4 mm, and the high current capability flexible graphite grounding material with a diameter of 28 mm which respectively containing 9 copper wires (1.4 mm in diameter) and 18 copper wires (1.0 mm in diameter). The copper wire adopts dispersive structure arrangement. The finite element method was used to calculate the equivalent impedance of the grounding electrode under the action of different frequency currents, and the corresponding result were extracted according to the amplitude and phase of the voltage and current. The external environment of the grounding electrode was air, and the initial temperature of the air is 25 °C. The calculation results are shown in Table 5.

From the calculation results, it can be seen that the copper wires in the flexible graphite grounding electrode adopted a decentralized structure design, which can greatly reduce the high frequency impedance and the short-time high current temperature rise dropped significantly at the same time. The high current capability flexible graphite grounding material had a good thermal stability compared with the steel material.

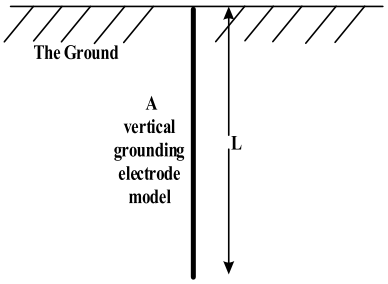

FIGURE 8. Diagram of the single vertical grounding electrode model.

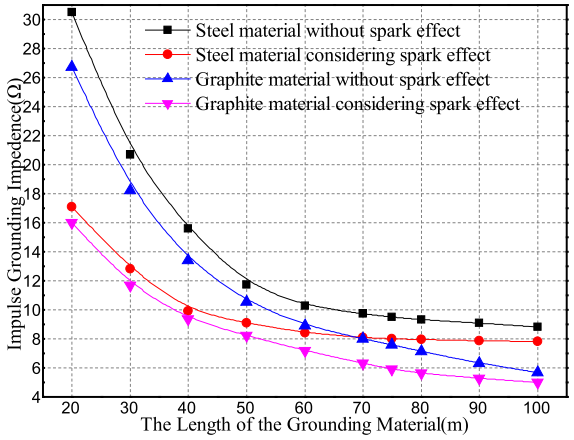

FIGURE 9. Diagram of the variation of grounding impedance of the single vertical grounding electrode with its length.

D. IMPULSE CURRENT EFFECTIVE LENGTH

Due to the end effect and inductance effect, the grounding electrode has an impulse current effective length when the impulse current scattering into the soil [14], [15]. However, the impulse grounding resistance is not linearly decreased when the power frequency grounding resistance decreases, and there is a saturation phenomenon [16]. Therefore, it is necessary to study the impulse current effective length of the high current capability flexible graphite grounding material. The parameter of the two materials are shown in Table 4. The amplitude and waveform of the lightning current was set to 30 kA and 8/20 μs respectively. The soil resistivity was 500 Ω·m. The calculation model was a single vertical grounding electrode is shown in Figure 8. The impulse grounding impedance changes with the length of the grounding electrode is shown in Figure 9.

In this paper, the impulse current effective length of the grounding material was defined as that when the derivative of impulse grounding resistance R_L to the length of grounding material L was less than one certain value.

$$-dR_{\mathrm{L}}/dL \leq \tan\alpha \tag{6}$$

where α is the angle between the tangent and the horizontal direction of the point on the curve that satisfies equation (6), and generally α takes as 5°, that is $\tan\alpha = 0.087$.

TABLE 6. Calculated results of the impulse current effective length.

Whether to considering the spark effect or not	Impulse current effective length (m)		Increase percentage
	Round Steel	Flexible graphite grounding material	
NOT	59.7	81.1	36%
YES	49.7	76.0	53%

Note: Increase percentage=(Impulse current effective length of the flexible graphite grounding material–Impulse current effective length of the round steel)/Impulse current effective length of the round steel ×100%

When the electric field strength exceeded the critical breakdown field strength of the soil, a partial spark discharge would occur, and the effect can be regarded as the size of the grounding electrode and the conductivity of the soil were increased. The relationship between the initial breakdown field strength E_0 of the soil and the resistivity ρ was given in reference [17].

$$E_0 = 241\rho^{0.215} \tag{7}$$

where E_0 is the critical breakdown field strength.

Based on the above definition, an iterative algorithm of equivalent radius was used to calculate the impulse current effective length of the flexible graphite grounding material and the steel grounding material under the condition of considering the spark effect or without spark effect [18]. The results are shown in Table 6.

When considering the spark effect, the impulse current effective length of the electrode was reduced, but the effective length increase percentage increased. The inductance effect of the round steel grounding material was stronger when considering the spark effect, which further hindered the current flowing to the distal end of the grounding material, resulting in a shorter impulse current effective length. The impulse current effective length of the flexible graphite grounding material was about 30% longer than that of the round steel grounding material.

IV. PRACTICAL ENGINEERING APPLICATION

The applications of the flexible graphite grounding material were currently available in 110 kV, 220 kV, 500 kV AC transmission towers, and ±800 kV, ±1100 kV DC transmission towers in China. The actual applications of the transmission tower grounding grids had been completed in some mountainous areas with serious corrosion, high lightning strike rate areas, and high soil resistivity areas. Good results of the practical engineering application had been achieved in typical soils such as saline-alkali soil, neutral meadow soil and acid red soil.

Figure 10 showed the diagram of the actual corrosion of the round steel grounding grid in a 220 kV and 500 kV transmission tower, as well as the schematic diagram of the actual engineered grounding grids using the scheme of laying the grounding electrode in the same ditch.

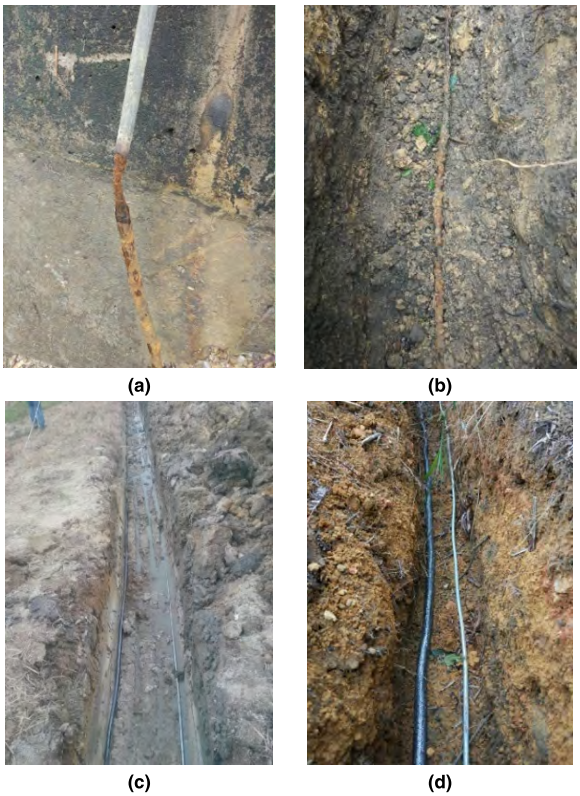

FIGURE 10. Practical engineering application of the graphite flexible grounding material. (a) Corrosion of the down lead line of round steel. (b) Corrosion of the round steel grounding grid. (c) Serious soil corrosion area. (d) High soil resistivity area.

TABLE 7. Comparison of the grounding resistance of the two typical tower grounding grids.

Transmission tower	Measurement results of the grounding resistance	
	Round steel	Graphite
a 220 kV transmission tower	9.9 Ω	7.6 Ω
a 500 kV transmission tower	4.6 Ω	3.1 Ω

The results in Table 7 showed that in the two typical transmission towers, the grounding resistance of the flexible graphite grounding grid was reduced by 23.23% and 32.61% respectively compared to the round steel grounding grid. To a certain extent, it showed that the flexible graphite grounding material had a reliable engineering application value.

V. CONCLUSION

The structure scheme of the flexible graphite grounding material proposed in this paper significantly enhanced its corrosion resistance, reduced its contact resistance with the soil, reduced the high-frequency impedance, and the short-time high-current temperature rise was also greatly reduced. The expected service life of the flexible graphite grounding

material can exceed 30 years. Under the condition of large soil particle size and high resistivity, the contact resistance of per unit area of the flexible graphite grounding material with the soil is reduced by about 30%. The impulse current effective length of the flexible graphite grounding material is more than 30% longer than that of the round steel grounding material. The flexible graphite grounding material has an important engineering application value for the long-term safety of the grounding system.

REFERENCES

[1] M. Apra, M. D'Amore, K. Gigliotti, M. S. Sarto, and V. Volpi, "Lightning indirect effects certification of a transport aircraft by numerical simulation," *IEEE Trans. Electromagn. Compat.*, vol. 50, no. 3, pp. 513–523, Aug. 2008.

[2] M. A. de Araujo, R. A. Flauzino, V. de Cillo Moro, and J. C. de Melo Vieira, Jr., "Modeling and simulation of surge arresters for lightning protection of distribution systems," *IEEE Latin Amer. Trans.*, vol. 13, no. 7, pp. 2225–2231, Jul. 2015.

[3] N. Asha, G. K. Manohar, K. K. Dani, and P. C. S. Devara, "A study of lightning activity over land and oceanic regions of India," *Earth Syst. Sci.*, vol. 118, no. 5, pp. 467–481, May 2009.

[4] C. Gomes and M. Z. A. A. Kadir, "Lightning protection: Getting it wrong," *IEEE Technol. Soc. Mag.*, vol. 30, no. 2, pp. 12–21, 2011.

[5] X. Zhang, "Computation of lightning transients in large scale multiconductor systems," *IEEE Access*, vol. 6, pp. 76573–76585, 2018.

[6] S. Tao, X. Zhang, Y. Wang, and J. Yang, "Transient behavior analysis of offshore wind turbines during lightning strike to multi-blade," *IEEE Access*, vol. 6, pp. 22070–22083, 2018.

[7] Y. Hu, J. Ruan, R. Gong, Z. Liu, Y. Wu, and W. Wen, "Flexible graphite composite electrical grounding material and its application in tower grounding grid of power transmission system," *Power Syst. Technol.*, vol. 38, no. 10, pp. 2851–2857, Oct. 2014.

[8] C. Xu and X. Hu, "Investigation of anti-corrosive metallic material for earthing grid," *Power Syst. Technol.*, vol. 27, no. 8, pp. 77–79, Aug. 2003.

[9] M. Tullmin and P. R. Roberge, "Corrosion of metallic materials," *IEEE Trans. Rel.*, vol. 44, no. 2, pp. 271–278, Jun. 1995.

[10] B. C. Syrett, J. A. Gorman, M. L. Arey, G. H. Koch, and G. A. Jacobson, "Cost of corrosion in the electric power industry," *Mater. Perform.*, vol. 41, no. 3, pp. 18–22, Feb. 2002.

[11] Y. Hu, J. Ruan, W. Xiao, Q. Zhan, D. Huang, and X. Wang, "Study on flexible graphite composite material for electrical grounding and its correlation experimentations," *High Voltage Eng.*, vol. 42, no. 6, pp. 1879–1889, Jun. 2016.

[12] R. Gong, J. Ruan, Y. Hu, H. Ge, and S. Jin, "Performance comparison between flexible graphite-copper composited grounding material and conventional grounding materials," presented at ICHVE, Chengdu, China, Dec, 2016, pp. 1–5. doi: 10.1109/ICHVE.2016.7800756.

[13] Y. Hu, Y. An, R. Xian, H. Li, J. Ruan, D. Huang, and W. Wen, "Study on magnetic properties of flexible graphite composite grounding material," presented at ICHVE, Chengdu, China, Dec, 2016, pp. 1–4. doi: 10.1109/ICHVE.2016.7800756.

[14] R. Zeng, X. Gong, J. He, B. Zhang, and Y. Gao, "Lightning impulse performances of grounding grids for substations considering soil ionization," *IEEE Trans. Power Del.*, vol. 23, no. 2, pp. 667–675, Feb. 2008.

[15] F. P. Dawalibi, W. Xiong, and J. Ma, "Transient performance of substation structures and associated grounding systems," *IEEE Trans. Ind. Appl.*, vol. 31, no. 3, pp. 520–527, May 1995.

[16] L. Grcev, "Impulse efficiency of ground electrodes," *IEEE Trans. Power Del.*, vol. 24, no. 1, pp. 441–451, Jan. 2009.

[17] E. E. Oettle, "A new general estimation carve for predicting the impedance' of concentrated Earth electrodes," *IEEE Trans. Power Del.*, vol. PWRD-3, no. 4, pp. 2020–2029, Apr. 1988.

[18] C. Zhang, Y. Gan, J. M. Zou, J. Ruan, and J. Xia, "Influences of spark effect and spark thorn on impulse grounding resistance of graphite grounding body," *Water Resour. Power*, vol. 35, no. 6, pp. 178–181, Jun. 2017.

DAOCHUN HUANG (S'08–M'10–SM'18) was born in Heilongjiang Province, China, in 1976. He received the B.S. degree in electrical engineering and its automation and the Ph.D. degree in high voltage and insulation technology from the School of Electrical Engineering, Wuhan University, Wuhan, China, in 2003 and 2009, respectively. He is currently an Associate Professor with the School of Electrical Engineering and Automation, Wuhan University. His research interests include the external insulation of transmission and transformation equipment, high-voltage apparatus, and the numerical analysis of electromagnetic field and its applications in engineering.

Dr. Huang is a member of the IEEE Dielectrics and Electrical Insulation Society and the International Council on Large Electric Systems (CIGRE).

JUN XIA was born in Henan, China, in 1992, He received the B.S. degree in electrical engineering and its automation from the School of Electrical Engineering, Wuhan University, China, in 2016, where he is currently pursuing the master's degree with the School of Electrical Engineering and Automation. His main research interests include new non-metal grounding material and its practical engineering applications, and the calculation of temperature field of high-voltage bushing.

JIANGJUN RUAN (M'03) was born in Zhejiang, China, in 1968. He received the B.S. and Ph.D. degrees in electric machine engineering from the Huazhong University of Science and Technology, Wuhan, China, in 1990 and 1995, respectively. He did his Postdoctoral Research from the Wuhan University of Hydraulic and Electric Engineering, Wuhan, in 1998. He is currently a Professor with Wuhan University, Wuhan. His research interests include electromagnetic field numerical simulation, high voltage and insulation technology, and the grounding technology.

YONGCONG WU was born in Guangdong, China, in 1991. He received the B.S. degree in electrical engineering and its automation from the School of Electrical Engineering and Automation, Wuhan University, Wuhan, China, in 2013, where he is currently pursuing the Ph.D. degree with the School of Electrical Engineering and Automation. His research interests include condition assessment of high-voltage switchgear, grounding technology, and multi-physics numerical simulation.

WANLIN QUAN was born in Hubei, China, in 1995. He received the B.S. degree in electrical engineering and its automation from Wuhan University, China, in 2017, where he is currently pursuing the master's degree with the School of Electrical Engineering and Automation. His main research interests include high voltage and insulation technology, numerical analysis, and engineering application of electromagnetic field.